

The AdS_4/CFT_3 algebraic curve

Nikolay Gromov ^{α} and Pedro Vieira ^{β}

^{α} *Service de Physique Théorique, CNRS-URA 2306 C.E.A.-Saclay, F-91191 Gif-sur-Yvette, France; Laboratoire de Physique Théorique de l'Ecole Normale Supérieure et l'Université Paris-VI, Paris, 75231, France; St.Petersburg INP, Gatchina, 188 300, St.Petersburg, Russia*
nikgromov@gmail.com

^{β} *Laboratoire de Physique Théorique de l'Ecole Normale Supérieure et l'Université Paris-VI, Paris, 75231, France; Departamento de Física e Centro de Física do Porto Faculdade de Ciências da Universidade do Porto Rua do Campo Alegre, 687, 4169-007 Porto, Portugal*
pedrogvieira@gmail.com

Abstract

We present the $OSp(2, 2|6)$ symmetric algebraic curve for the AdS_4/CFT_3 duality recently proposed in arXiv:0806.1218. It encodes all classical string solutions at strong t'Hooft coupling and the full two loop spectrum of long single trace gauge invariant operators in the weak coupling regime. This construction can also be used to compute the complete superstring semi-classical spectrum around any classical solution. We exemplify our method on the BMN point-like string.

1 Introduction and main results

In [1] integrability emerged once again [2] in the study of superconformal gauge theories. In this work Minahan and Zarembo wrote down a set of five Bethe equations yielding the complete 2-loop spectrum of the three dimensional superconformal $SU(N) \times SU(N)$ Chern-Simons theory recently proposed by Aharony, Bergman, Jafferis and Maldacena in [3] following [4]. This theory was conjectured in [3] to be the effective theory for a stack of M2 branes at a Z_k orbifold point. In the large N limit, the gravitational dual becomes M-theory on $AdS_4 \times S^7/Z_k$. For large k and N with

$$\lambda = N/k \equiv 8g^2 \tag{1.1}$$

fixed, the dual theory becomes type IIA superstring theory in $AdS_4 \times CP^3$. For subsequent interesting works see [5, 6, 1, 7, 8]. In [7],[8] the superstring coset sigma model was constructed and shown to be classically integrable.

In this paper we present the algebraic curve construction for the AdS_4/CFT_3 duality at weak and strong coupling. The curves we present encode the full 2-loop spectrum of long single trace gauge invariant operators in the ABJM Chern Simons theory and the complete classical motion of free type IIA superstring theory in $AdS_4 \times CP^3$. The curve for the AdS_5/CFT_4 Maldacena duality was considered in [9, 10, 11, 12, 13, 14].

For the string side we have a supercoset sigma model whose target space is

$$\frac{OSp(2, 2|6)}{SO(3, 1) \times SU(3) \times U(1)} \tag{1.2}$$

which has $AdS_4 \times CP^3$ as its bosonic part. The algebraic curves allow us to map each classical solution to a corresponding Riemann surface which encodes an infinite set of conserved charges particular to the classical solution in study. The map goes as follows. Given a classical solution we can diagonalize the monodromy matrix

$$\Omega(x) = P \exp \int d\sigma J_\sigma(x) \tag{1.3}$$

where $J(x)$ is the flat connection, present for integrable theories and computed for the model in study in [7, 8] and for the $AdS_5 \times S^5$ superstrings in [15]. The eigenvalues of such matrix (as of any generic matrix) live in a Riemann surface whose size is roughly speaking the size of the matrix¹. In our case, as explained below, we will see that the logarithms of these eigenvalues can be organized into a 10-sheeted Riemann surface whose properties are listed below.

Turning the logic around, the algebraic curve construction allows one to trade the study of the intricate non-linear equations of motion by the construction of Riemann surfaces with some precise prescribed analytical properties. The string dynamics can be translated to the study of analytical properties of algebraic curves, a well developed subject in algebraic geometry.

To illustrate what we mean let us describe the algebraic curve studied in this paper. To find the complete classical spectrum of the theory we should proceed as follows: We should build ten-sheeted Riemann surfaces whose branches², called quasi-momenta, depend on a spectral

¹For some matrices, such as for example elements of $SO(2N + 1)$, some eigenvalues might be trivial.

²Actually as will become clear later the quasi-momenta define an infinite genus curve and to obtain a ten-sheeted Riemann surface we should take for example the derivative of this quasimomenta w.r.t. x .

which roughly speaking measures how big the cut is. (From the point of view of the classical solutions these are the action variables.)

3. The quasi-momenta must behave as

$$\begin{pmatrix} q_1(x) \\ q_2(x) \\ q_3(x) \\ q_4(x) \\ q_5(x) \end{pmatrix} = - \begin{pmatrix} q_{10}(x) \\ q_9(x) \\ q_8(x) \\ q_7(x) \\ q_6(x) \end{pmatrix} \simeq \frac{1/2}{x \pm 1} \begin{pmatrix} \alpha_{\pm} \\ \alpha_{\pm} \\ \alpha_{\pm} \\ \alpha_{\pm} \\ 0 \end{pmatrix} \quad (1.6)$$

close to the singular points $x = \pm 1$. The constant α_{\pm} has no significance from the target space point of view, the only think we should keep in mind is that the residues must be synchronized (Physically this is a manifestation of the Virasoro constraints imposed on the classical solutions).

4. The curve should possess the inversion symmetry

$$\begin{pmatrix} q_1(1/x) \\ q_2(1/x) \\ q_3(1/x) \\ q_4(1/x) \\ q_5(1/x) \end{pmatrix} = \begin{pmatrix} 0 \\ 0 \\ 2\pi m \\ 2\pi m \\ 0 \end{pmatrix} + \begin{pmatrix} -q_2(x) \\ -q_1(x) \\ -q_4(x) \\ -q_3(x) \\ +q_5(x) \end{pmatrix} = \begin{pmatrix} 0 \\ 0 \\ 2\pi m \\ 2\pi m \\ 0 \end{pmatrix} + \begin{pmatrix} +q_9(x) \\ +q_{10}(x) \\ +q_7(x) \\ +q_8(x) \\ -q_6(x) \end{pmatrix} \quad (1.7)$$

with m being an integer.

5. Finally the large x asymptotics of the Riemann surface read³

$$\begin{pmatrix} q_1(x) \\ q_2(x) \\ q_3(x) \\ q_4(x) \\ q_5(x) \end{pmatrix} = \begin{pmatrix} q_{10}(x) \\ q_9(x) \\ q_8(x) \\ q_7(x) \\ q_6(x) \end{pmatrix} \simeq \frac{1}{2gx} \begin{pmatrix} L + E + S \\ L + E - S \\ L - M_r \\ L + M_r - M_u - M_v \\ M_v - M_u \end{pmatrix}. \quad (1.8)$$

Therefore, if we enumerate all possible Riemann surfaces with the properties just listed, then, it suffices to evaluate the quasimomenta at large values of the spectral parameter to obtain the energy spectrum of all classical string solutions as a function of the global charges charges and several moduli of the algebraic curve.

Notice that each cut of the algebraic curve is characterized by a discrete label (i, j) , corresponding to the two sheets being united, an integer n , the multiple of 2π mentioned above, and a real filling fraction. These three quantities are the analogues of the polarization, mode number and amplitude of the flat space fourier decomposition of a given classical solution.

Then we have a clear geometrical picture of semi-classical quantization in the context of these algebraic curves. Namely a classical solution will be represented as some algebraic curve

³The state labeled by (M_u, M_r, M_v) belongs to the $SU(4)$ representation with Dynkin labels $[L - 2M_u + M_r, M_u + M_v - 2M_r, L - 2M_v + M_r]$

with same large cuts uniting several pairs of sheets. Quantum fluctuations correspond to adding small singularities – microscopic cuts or poles – to this Riemann surface [16]. The different choices of sheets to be connected in this way correspond to the different string polarizations we can excite. We will exemplify this procedure on the example of the simplest classical solution – the BMN [17] string studied in the present framework in [6]. This method can be easily generalized to more complicated solutions and to the study of the ground state energy around any classical solution [18].

One needs to carry on the investigation of integrability in *AdS/CFT*, so successful for the most famous *AdS₅/CFT₄* duality [19]. The results are of course unpredictable but one thing can be taken for granted – the understanding of the integrable structures behind all these beautiful theories can only deepen our understanding of non-perturbative gauge theories and theories of quantum gravity.

2 String algebraic curve

In this paper we analyze the algebraic curve for free type IIA superstrings in *AdS₄/CP³*. To compute the algebraic curve we could use the flat connection in [7, 8] which has superficially the same form as that found by Benna Polchinski and Roiban for the *AdS₅ × S⁵* strings [15]. Armed with the experience of what happens in the *AdS₅/CFT₄* duality [9, 14, 16] we follow a shortcut. We shall use the purely bosonic part of the action to compute the *CP³* and the *AdS₄* algebraic curves. Only Virasoro will couple them. Then, to lift it from the classical bosonic curve to the complete semi-classical curve for the full super group, we will simply allow the several sheets of the two curves to be connected by further small cuts or poles. If the poles connect *CP³* sheets with *AdS₄* sheets then we will be studying the missing fermionic excitations. Of course, if we would proceed as in [14] using the full flat connection in [7, 8] we would find exactly the same results as can be easily checked.

Technically, our treatment is very similar to the one in [11] where the *SO(6)* bosonic string was studied and the generalization to *SO(2n)* was carried on. This is not surprising since *OSp(2, 2|6)* is not very different from *SO(10)*.

2.1 Bosonic flat connection

The bosonic part of the *AdS₄/CP³* type IIA free superstring theory reads

$$S = \sqrt{2\lambda} \int d\sigma d\tau (\mathcal{L}_{CP^3} + \mathcal{L}_{AdS^4}) \quad (2.1)$$

where

$$\mathcal{L}_{AdS^4} = -\frac{1}{4} (\partial_\mu n \cdot \partial_\mu n - \Lambda (n \cdot n - 1)) , \quad (2.2)$$

and

$$\mathcal{L}_{CP^3} = (D_\mu z)^\dagger \cdot D_\mu z - \Lambda' (z^\dagger \cdot z - 1) . \quad (2.3)$$

Here n and z are vectors made out of the embedding coordinates of the anti de-Sitter and the projective space. Thus

$$n = (n_1, \dots, n_5) , \quad n \cdot n = n_1^2 + n_2^2 - n_3^2 - n_4^2 - n_5^2 \quad (2.4)$$

with n_i real while

$$z = (z^1, \dots, z^4), \quad z^\dagger \cdot z = |z^1|^2 + \dots + |z^4|^2 \quad (2.5)$$

where z^I are complex numbers. In what follows whenever the index structure is obvious we omit it. The z^I are also identified up to a phase, $z^I \simeq e^{i\varphi} z^I$. This $U(1)$ gauge symmetry is accounted by the gauge field A_μ appearing in

$$D_\mu z = \partial_\mu z + iA_\mu z. \quad (2.6)$$

The equations of motion for the connection yield $z \cdot (D_\mu z)^\dagger - (D_\mu z) \cdot z^\dagger = 0$ while the constrain $\partial_\mu(z^\dagger \cdot z) = 0$ yields $z \cdot (D_\mu z)^\dagger + (D_\mu z) \cdot z^\dagger = 0$ and therefore, on-shell, we have separately

$$(D_\mu z) \cdot z^\dagger = z \cdot (D_\mu z^\dagger) = 0. \quad (2.7)$$

Analogously, for the n field we have

$$n \cdot (\partial_\mu n) = 0. \quad (2.8)$$

Next it is useful to introduce the element

$$h = \left(\frac{1 - 2z^\dagger \otimes z}{1 - 2n \otimes n} \right) \Leftrightarrow h_{AB} = \left(\frac{\delta_I^J - 2z_I^\dagger z^J}{\delta_{ij} - 2n_i n_j} \right), \quad (2.9)$$

and the connection

$$j = h^{-1} dh. \quad (2.10)$$

It is easy to see that when $z^\dagger \cdot z = n \cdot n = 1$ and (2.7), (2.8) hold we have

$$j_{AB} = \left(\frac{j_{\text{AdS}}}{j_{\text{CP}}} \right) = 2 \left(\frac{n_i (\partial_\mu n_j) - (\partial_\mu n_i) n_j}{z_I^\dagger (D_\mu z)^J - (D_\mu z)_I^\dagger z^J} \right) \quad (2.11)$$

and the action becomes

$$S = -\frac{g}{4} \int d\sigma d\tau \text{STr}_{\text{OSp}}(j_\mu^2). \quad (2.12)$$

where⁴

$$\text{STr}_{\text{OSp}}(j^2) \equiv -\frac{1}{2} \text{Tr}(j_{\text{AdS}}^2) + 2 \text{Tr}(j_{\text{CP}}^2) \quad (2.13)$$

Note also that the Virasoro constraint now implies

$$\text{STr}_{\text{OSp}}(j_1 \pm j_0)^2 = 0. \quad (2.14)$$

At this point, we have the flatness condition

$$dj + j \wedge j = 0, \quad (2.15)$$

⁴The reason for this definition lies in the relations between quadratic Casimirs for $SO(5)$, $Sp(4)$ and $SU(4)$, $SO(6)$

$$\text{Tr}_{SO(5)}(j^2) = 2 \text{Tr}_{Sp(4)}(j^2), \quad \text{Tr}_{SU(4)}(j^2) = \frac{1}{2} \text{Tr}_{SO(6)}(j^2)$$

following from the expression (2.10) of the connection, and

$$d * j = 0, \tag{2.16}$$

encoding the equations of motion for both the n and the z field. These two equations follow from the flatness condition for the Lax connection

$$J(x) = \frac{j + x * j}{1 - x^2} \tag{2.17}$$

as can be easily checked by collecting powers of x . The new variable x appearing in (2.17) is a completely arbitrary complex number called spectral parameter. Using this flat connection we can build the monodromy matrix

$$\Omega(x) = P \exp \int d\sigma J_\sigma(x) \tag{2.18}$$

where we integrate over a constant τ worldsheet loop. At this point integrability comes into stage. The connection being flat, the eigenvalues of the monodromy matrix are independent of τ and since moreover they depend on a generic complex number x they define an infinite set of conserved charges. For example, each coefficient in the Taylor expansion of the eigenvalues around a particular point x^* is a conserved charge. The existence of this large number of conserved charges render the sigma model (at least classically) integrable.

We want to study the algebraic curve construction for this integrable model. This will map each classical string solution to a Riemann surface with precise analytical properties. The study of classical solutions in $AdS_4 \times CP^3$ can then be reduced to the problem of making a catalogue of all Riemann surfaces compatible with the prescribed analytical properties.

2.2 The $AdS_4 \times CP^3$ algebraic curve

In this section we study the eigenvalues of the monodromy matrix (2.18). We will first consider purely bosonic solutions and work out the full supercurve in the next section. From the form of the flat connection, in particular from the fact that each of the blocks in (2.11) is manifestly traceless, we find that the connection is explicitly block diagonal and thus its eigenvalues will split into two groups: The eigenvalues coming from the CP^3 part

$$\{e^{i\tilde{p}_1}, \dots, e^{i\tilde{p}_4}\}, \tag{2.19}$$

with

$$\tilde{p}_1(x) + \dots + \tilde{p}_4(x) = 0, \tag{2.20}$$

and those coming from the diagonalization of the AdS block,

$$\{e^{i\hat{p}_1}, \dots, e^{i\hat{p}_4}, 1\}, \tag{2.21}$$

where moreover

$$\hat{p}_3(x) + \hat{p}_2(x) = 0 = \hat{p}_4(x) + \hat{p}_1(x). \tag{2.22}$$

To find the eigenvalues of the monodromy matrix we solve a polynomial characteristic equation. This defines an algebraic curve for the eigenvalues λ . Thus, the eigenvalues can be thought of as different branches of the same Riemann surfaces with square root cuts uniting the several sheets. For example when crossing a cut \mathcal{C} shared by the eigenvalues $e^{i\hat{p}_1}$ and $e^{i\hat{p}_2}$ we simply change Riemann sheet,

$$(e^{i\hat{p}_2})^+ - (e^{i\hat{p}_1})^- = 0, \quad x \in \mathcal{C} \quad (2.23)$$

where the superscript \pm indicates the function is evaluated immediately above/below the cut. The quasi-momenta on the other hand are not exactly the eigenvalues but rather the logarithms of the eigenvalues. Thus when crossing the very same cut the quasimomenta will in general also gain an integer multiple of 2π ,

$$\hat{p}_2^+ - \hat{p}_1^- = 2\pi n, \quad x \in \mathcal{C}. \quad (2.24)$$

In general we can have several cuts uniting different pairs of sheets and

$$p_i^+ - p_j^- = 2\pi n, \quad x \in \mathcal{C}_{ij}, \quad (2.25)$$

on each cut connecting two quasimomenta p_i and p_j . To parametrize each cut we also introduce the usual filling fractions

$$\hat{S}_{ij} = \frac{g}{2\pi i} \oint_{\mathcal{C}_{ij}} dx \left(1 - \frac{1}{x^2}\right) \hat{p}_i(x), \quad \tilde{S}_{ij} = \frac{g}{\pi i} \oint_{\mathcal{C}_{ij}} dx \left(1 - \frac{1}{x^2}\right) \tilde{p}_i(x) \quad (2.26)$$

for the cuts uniting p_i and p_j . Each cut of the algebraic curve is characterized by a discrete label (i, j) , corresponding to the two sheets being united, an integer n , the multiple of 2π mentioned above, and a real filling fraction. These three quantities are the analogues of the polarization, mode number and amplitude of the flat space Fourier decomposition of a given classical solution.

The study of the analytical properties of the quasi-momenta follows closely the analysis done in the context of the AdS_5/CFT_4 duality in [14]. Let us enumerate all these properties and then explain their origin.

For large values of the spectral parameter, the quasimomenta behave as

$$\begin{aligned} (\hat{p}_1, \hat{p}_2, \hat{p}_3, \hat{p}_4) &\simeq \frac{1}{gx} (L + E, S, -S, -L - E), \\ (\tilde{p}_1, \tilde{p}_2, \tilde{p}_3, \tilde{p}_4) &\simeq \frac{1}{2gx} (L - M_u, M_u - M_r, M_r - M_v, -L + M_v), \end{aligned} \quad (2.27)$$

for a state belonging to the $SU(4)$ representation with Dynkin labels $[L - 2M_u + M_r, M_u + M_v - 2M_r, L - 2M_v + M_r]$ (which should be positive).

There are two simple poles at $x = \pm 1$ which are synchronized between the AdS_4 and the CP^3 quasi-momenta,

$$(\hat{p}_1, \hat{p}_2, \hat{p}_3, \hat{p}_4; \tilde{p}_1, \tilde{p}_2, \tilde{p}_3, \tilde{p}_4) \simeq \frac{1}{x \pm 1} \left(\alpha_{\pm}, 0, 0, -\alpha_{\pm}; \frac{\alpha_{\pm}}{2}, 0, 0, -\frac{\alpha_{\pm}}{2} \right), \quad (2.28)$$

and finally the algebraic surface exhibits a $x \rightarrow 1/x$ inversion symmetry under which

$$\begin{aligned} \hat{p}_1(1/x) &= -\hat{p}_1(x) & \tilde{p}_1(1/x) &= \tilde{p}_4(x) + 2\pi m \\ \hat{p}_2(1/x) &= +\hat{p}_2(x) & \tilde{p}_2(1/x) &= \tilde{p}_2(x) \\ \hat{p}_3(1/x) &= +\hat{p}_3(x) & \tilde{p}_3(1/x) &= \tilde{p}_3(x) \\ \hat{p}_4(1/x) &= -\hat{p}_4(x) & \tilde{p}_4(1/x) &= \tilde{p}_1(x) - 2\pi m \end{aligned} \quad (2.29)$$

with m being an integer dependent on the classical solution to which these quasi-momenta are associated.

Let us now briefly explain the origin of these analytical properties. The fact that the quasi-momenta encode the global charges of the classical solutions at the $x \rightarrow \infty$ asymptotics follows from the large x behavior of the monodromy matrix,

$$\Omega(x) \simeq 1 + \frac{1}{x} \int d\sigma j_\tau. \quad (2.30)$$

From the form of the flat connection we see that in general the quasi-momenta can have simple poles at $x = \pm 1$. The reason why only four of them – two in CP^3 and two in AdS_4 – have non-vanishing residues follows from the very particular form of the flat connection. For example for $x \simeq 1$ we have $J(x) \propto j_+$ and thus

$$j_+ \cdot v = 0 \quad (2.31)$$

if v is orthogonal to both z_I^\dagger , $D_+ z_I^\dagger$, n_i and $\partial_+ n_i$. Following the arguments in [11], this can be shown to imply that only two CP^3 and two AdS_4 quasimomenta have poles. Since moreover (2.20) and (2.22) we immediately see that the residues at these poles must be symmetric. Moreover the Virasoro constraints $\text{STr}(j_\mu^2) = 0$ synchronizes the poles in the anti de-Sitter and projective space as in (2.28) (exactly as in [13]).

Next we notice that $h^{-1} = h$. This has important consequences for the algebraic curve. It implies that

$$\Omega(x) = h^{-1}(2\pi)\Omega(1/x)h(0) \quad (2.32)$$

and therefore the eigenvalues of the monodromy matrix associated to some closed string classical solution are at most exchanged between themselves under the inversion map $x \rightarrow 1/x$. The precise way in which the quasi-momenta are exchanged is in general a subtle business [11, 13]. For example, a priori from (2.32) it seems that we could not infer that $\tilde{p}_2(1/x)$ is not exchanged with $\tilde{p}_3(x)$ for example. The reason why this can not happen and the inversion symmetry we postulated is OK is the following: There are solutions with $z_1, z_2, z_3 \neq 0$ but $z_4 = 0$. For those solutions the last line and column of the current $J(x)$ is made out of zeros. Thus $\Omega(x)$ will have one eigenvalue exactly equal to 1. In other words, one of the quasimomenta is strictly zero. Since \tilde{p}_1 and \tilde{p}_4 have poles this quasimomenta must be either \tilde{p}_2 or \tilde{p}_3 . But then, if for example $\tilde{p}_3 = 0$ while the other three quasimomenta are nontrivial vanishing then, clearly, $p_2(1/x) \neq p_3(x)$! In the same way we can justify the remaining relations in (2.29)⁵.

⁵As we mentioned in the beginning we could also have constructed the curve using the flat connection in [7, 8]. The $x \rightarrow 1/x$ symmetry we just discussed appears in these works as a consequence of the \mathbb{Z}_4 grading of the superalgebra (see equation at the end of section 4.1 in [8]). In the context of the $AdS_5 \times CFT_4$ correspondence – see [13] – this was also the case. Had we used the flat connections in these works and we would have found the same inversion symmetry properties.

2.3 Full algebraic supercurve

In this section we generalize the classical bosonic algebraic curve described in the previous section to the semi-classical and supersymmetric $OSp(2, 2|6)$ algebraic curve. The smallest representation of this symmetry group – which behaves in many aspects as $SO(10)$ – is **10** dimensional so we should find a nice linear combination of the quasimomenta in the previous section yielding **10** functions describing a single algebraic curve with manifest $OSp(2, 2|6)$ symmetry. Then, to include fermions, we simply allow for extra poles between the AdS_4 and the CP^3 quasimomenta! A proper linear combination is the following reorganization of the quasimomenta into a set of ten functions

$$\{q_1, q_2, q_3, q_4, q_5\} = \left\{ \frac{\hat{p}_1 + \hat{p}_2}{2}, \frac{\hat{p}_1 - \hat{p}_2}{2}, \tilde{p}_1 + \tilde{p}_2, \tilde{p}_1 + \tilde{p}_3, \tilde{p}_1 + \tilde{p}_4 \right\}, \quad (2.33)$$

and

$$\{q_6, q_7, q_8, q_9, q_{10}\} = -\{q_1, q_2, q_3, q_4, q_5\}. \quad (2.34)$$

These ten functions can be thought of as the several sheets of a single function taking values in a ten-sheeted Riemann surface as represented in figure 1. Notice that they organize in a nice explicitly $OSp(2, 2|6)$ symmetric way. From the properties derived in the previous section the properties for the q_i listed in the introduction follow. In particular we have (1.6), (1.7) and (1.8).

Next, to understand the quasi-classical quantization of any classical solution we add extra pole singularities to the different pairs of sheets of the algebraic curve associated with the solution we want to quantize. The several pairs of sheets to be connected in figure 1 correspond to the different physical polarizations for the quantum fluctuations. Thus, we are in need of a map between the several possible excitations of the string Hilbert space (or of the dual gauge theory) and the several pairs or Riemann surfaces.

This map is provided by figure 2 where we listed all $16 = 8 + 8$ physical excitations. The fluctuations are identified by the corresponding excitations of the $OSp(2, 2|6)$ Dynkin diagram with Dynkin labels as in [1]. Since the asymptotics of the curve can also be related to the Dynkin labels of a given state this suffices to identify which pairs of sheets are connected for each quantum fluctuation. See [13, 16] for similar analysis in the context of the AdS_5/CFT_4 duality.

In the next section we will explicitly apply figure 2 to the semi-classical quantization of the BMN string.

2.4 BMN string

The BMN point-like string has $z_1 = \frac{1}{\sqrt{2}}e^{i\omega\tau/2}$, $z_2 = \frac{1}{\sqrt{2}}e^{-i\omega\tau/2}$ and $n_1 + in_2 = e^{i\omega\tau}$. Computing the charges of this solution we find

$$L = 4\pi g\omega = \pi\sqrt{2\lambda}\omega, \quad E = 0 \quad (2.35)$$

to check that one can use that the AdS_5 time is given by $-i\log(n_1 + in_2)$. To compare the results we will find below with those in [6] we notice that

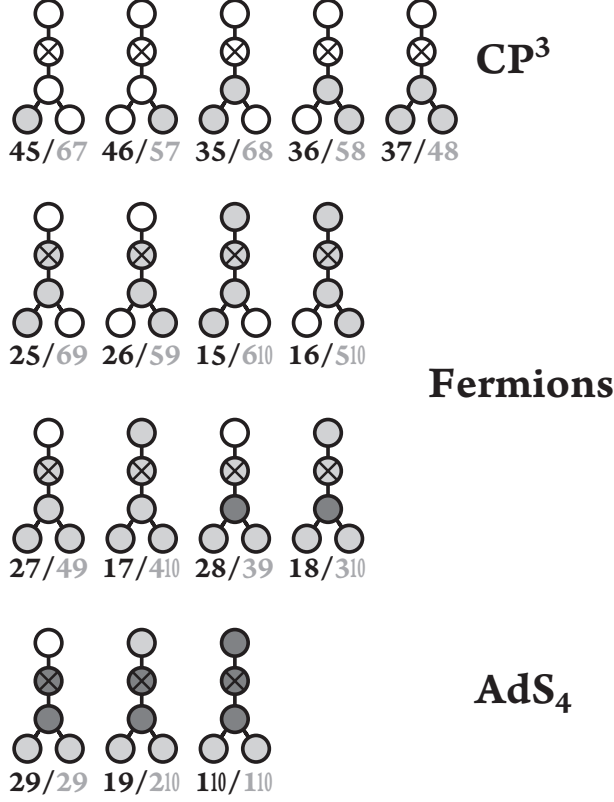


Figure 2: The several states in the Hilbert space can be constructed in the usual oscillator representation. There is one oscillator per Dynkin node of the $OSp(2, 2|6)$ super Dynkin diagram. A light (dark) gray shaded node corresponds to an oscillator excited once (twice). From the Chern-Simons Bethe ansatz point of view, the number of times each oscillator is excited is the same as the number of Bethe roots of the corresponding type. Thus, for example, in the notation of [1], the last fermionic excitation corresponds to a bound state of one root of each type u, v, w, s and two Bethe roots r . From the string point of view fluctuations correspond to poles uniting the several sheets of the algebraic curve. Close to each fluctuation we represented some numbers like 45/67 for the first fluctuation. They indicate which momenta are being united by this pole. In this case it is momenta q_4 and q_5 . Since (2.34) automatically q_6 and q_7 also share a pole.

$$\frac{n^2}{\omega^2} = \frac{2\pi^2 \lambda n^2}{L^2}. \quad (2.36)$$

We now plug the embedding coordinates into (2.11) and compute the path ordered exponential in (2.18). Since the string is point-like there is no σ dependence and this computation is trivial. We can then compute the eigenvalues of the monodromy matrix (2.18) and from them we find the $\mathbf{10}$ q_i 's using (2.33) and (2.34). We obtain

$$q_{1,\dots,4} = -q_{6,\dots,10} = \frac{2\pi\omega x}{x^2 - 1}, \quad (2.37)$$

and

$$q_{5,6} = 0. \quad (2.38)$$

The BMN string is the simplest possible algebraic curve. It is in fact the *vacuum curve*, all sheets are empty except for the two single poles at $x = \pm 1$.

We can now exemplify the computation of the quasi-classical spectrum in the algebraic curve language and reproduce the recent results of [6]. The 16 physical excitations are represented in figure 2. Notice that the first four CP^3 fluctuations and the last four fermionic fluctuations corresponds to poles shared by a quasimomenta in the list (2.37) with one of the two quasimomenta in (2.38). The position of these fluctuations is given by [16]

$$q_i(x_n) - q_j(x_n) = 2\pi n. \quad (2.39)$$

The integer n is the generalization of the Fourier mode in flat space – it is meaningful around any classical solution, no matter how non-linear and non-trivial this solution might be. For the fluctuations we are discussing this equation reads

$$\frac{2\pi\omega x_n}{x_n^2 - 1} = 2\pi n, \quad (2.40)$$

and we should pick the solution in the physical region $|x| > 1$. On the other hand all the remaining eight fluctuations connect two quasimomenta in (2.37). Therefore, from (2.39), we will find that the position of these fluctuations is fixed by

$$\frac{2\pi\omega x_n}{x_n^2 - 1} = \pi n. \quad (2.41)$$

So the position of half of the fluctuations is the same as the position of the other half with doubled mode number. This already points towards the structure of the fluctuation energies observed in [6]. We also recall that a fluctuation pole at position y should have a residue [16]

$$\alpha(y) = \frac{1}{2g} \frac{y^2}{y^2 - 1} \quad (2.42)$$

We will now consider separately the CP^3 , AdS_4 and Fermionic excitations to understand how to compute the fluctuation energies around a classical solution in the algebraic curve formalism. The computations are conceptually as in [16] so we will simply present the results for the perturbed quasi-momenta with very few explanations.

A technical detail: When computing the fluctuation spectrum we will add always a fluctuation with mode number n and another with mode number $-n$ to keep the string total world-sheet momentum zero in the process. We could alternatively excite all polarizations at the same time while obeying the level matching condition

$$\sum_{ij,n} n N_n^{ij} = 0, \quad (2.43)$$

with N_n^{ij} being the number of fluctuations with polarization (i, j) and mode number n . This would lead to the same results but with cluster our expression so we will chose to add always a single pair of fluctuations at a time.

2.4.1 CP^3 excitations

There are two types of fluctuations in CP^3 : The first four in figure 2 and the fifth one. The former corresponds to a pole connecting a quasi-momenta in (2.37) with an empty one in (2.38) whereas the latter corresponds to a pole shared by q_3 and q_7 , both in (2.37). Let us consider one of the fluctuations of the first type, say the first one in figure 2. For this fluctuation

$$\delta q_3 = -\delta q_8 = + \sum_{\pm} \frac{\alpha(1/x)}{1/x - x_{\pm n}} \quad (2.44)$$

$$\delta q_4 = -\delta q_7 = - \sum_{\pm} \frac{\alpha(x)}{x - x_{\pm n}} \quad (2.45)$$

$$\delta q_5 = -\delta q_6 = + \sum_{\pm} \frac{\alpha(x)}{x - x_{\pm n}} + \sum_{\pm} \frac{\alpha(1/x)}{1/x - x_{\pm n}} \quad (2.46)$$

$$\delta q_{1,2} = -\delta q_{9,10} = + \frac{\alpha(x) \delta E}{x}. \quad (2.47)$$

so that from the synchronization of poles at $x = \pm 1$ we find

$$\delta E = \sum_{\pm} \frac{1}{x_{\pm n}^2 - 1} = \sum_{\pm n} \sqrt{\frac{1}{4} + \frac{n^2}{\omega^2}} - \frac{1}{2}. \quad (2.48)$$

The fifth fluctuation in CP^3 connects q_3 and q_7 (and therefore automatically at $q_4 = -q_7$ and $q_8 = -q_3$) so we have

$$\delta q_4 = -\delta q_7 = - \sum_{\pm} \frac{\alpha(x)}{x - x_{\pm n}} + \sum_{\pm} \frac{\alpha(1/x)}{1/x - x_{\pm n}} \quad (2.49)$$

$$\delta q_3 = -\delta q_8 = - \sum_{\pm} \frac{\alpha(x)}{x - x_{\pm n}} + \sum_{\pm} \frac{\alpha(1/x)}{1/x - x_{\pm n}} \quad (2.50)$$

$$\delta q_{1,2} = -\delta q_{9,10} = + \frac{\alpha(x) \delta E}{x}. \quad (2.51)$$

and we find in this case

$$\delta E = \sum_{\pm} \frac{2}{x_{\pm n}^2 - 1} = \sum_{\pm n} \sqrt{1 + \frac{n^2}{\omega^2}} - 1. \quad (2.52)$$

These are precisely the results of [6].

2.4.2 AdS^4 excitations

Here we must be careful. The first and third AdS^4 fluctuations have two excitations in the last Dynkin node – see figure 2. This means that for those we should double the residue (2.42). Let

us consider the last one for illustration (for the first one we get the same result of course). We have

$$\delta q_1 = -\delta q_{10} = + \sum_{\pm} \frac{2\alpha(x_n)}{x - x_{\pm n}} \quad (2.53)$$

$$\delta q_2 = -\delta q_9 = - \sum_{\pm} \frac{2\alpha(x_n)}{1/x - x_{\pm n}} \quad (2.54)$$

and thus, from the large x asymptotics,

$$\delta E = \sum_{n=\pm} \frac{x_n^2 + 1}{x_n^2 - 1} = \sum_{\pm n} \sqrt{1 + \frac{n^2}{\omega^2}}. \quad (2.55)$$

As for the middle fluctuation in figure 2, we have

$$\delta q_1 = -\delta q_{10} = + \sum_{\pm} \frac{\alpha(x_n)}{x - x_{\pm n}} - \sum_{\pm} \frac{\alpha(x_n)}{1/x - x_{\pm n}} \quad (2.56)$$

$$\delta q_2 = -\delta q_9 = + \sum_{\pm} \frac{\alpha(x_n)}{x - x_{\pm n}} - \sum_{\pm} \frac{\alpha(x_n)}{1/x - x_{\pm n}} \quad (2.57)$$

yielding

$$\delta E = \sum_{n=\pm} \frac{x_n^2 + 1}{x_n^2 - 1} = \sum_{\pm n} \sqrt{1 + \frac{n^2}{\omega^2}} \quad (2.58)$$

which is again the same result as found in [6].

2.4.3 Fermionic excitations

As for CP^3 here we also have two types of fluctuations corresponding to the first and second lines in figure 2. We start by considering a representative of the first line. For example let us focus on a pole from q_1 to q_5 (and thus automatically also from q_6 to q_{10}). We have

$$\delta q_1 = -\delta q_{10} = + \sum_{\pm} \frac{\alpha(x_n)}{x - x_{\pm n}} \quad (2.59)$$

$$\delta q_5 = -\delta q_6 = - \sum_{\pm} \frac{\alpha(x_n)}{x - x_{\pm n}} - \sum_{\pm} \frac{\alpha(x_n)}{1/x - x_{\pm n}} \quad (2.60)$$

$$\delta q_2 = -\delta q_9 = - \sum_{\pm} \frac{\alpha(x_n)}{1/x - x_{\pm n}} \quad (2.61)$$

giving

$$\delta E = \sum_{n=\pm} \frac{x_n^2 + 1}{2(x_n^2 - 1)} = \sum_{\pm n} \sqrt{\frac{1}{4} + \frac{n^2}{\omega^2}} \quad (2.62)$$

For a fluctuation in the second line, say the last one, we have

$$\delta q_1 = -\delta q_{10} = -\sum_{\pm} \frac{\alpha(x_n)}{x - x_{\pm n}} - \frac{Ax}{2g(x^2 - 1)} \quad (2.63)$$

$$\delta q_2 = -\delta q_9 = +\sum_{\pm} \frac{\alpha(x_n)}{1/x - x_{\pm n}} - \frac{Ax}{2g(x^2 - 1)} \quad (2.64)$$

$$\delta q_3 = -\delta q_8 = +\sum_{\pm} \frac{\alpha(x)}{x - x_{\pm n}} \quad (2.65)$$

$$\delta q_4 = -\delta q_7 = -\sum_{\pm} \frac{\alpha(1/x)}{1/x - x_{\pm n}} \quad (2.66)$$

so that pole synchronization gives

$$A = \sum_{\pm} \frac{1}{x_{\pm n}^2 - 1} \quad (2.67)$$

and then from the large x asymptotics we read the energy shift

$$\delta E = \sum_{\pm n} \frac{x_n^2 + 3}{2(x_n^2 - 1)} = \sum_{\pm n} \sqrt{1 + \frac{n^2}{\omega^2}} - \frac{1}{2} \quad (2.68)$$

This completes the computation of the spectrum of the superstring around the BMN classical solution. All frequencies coincide with those found in [6].

3 Chern-Simons curve

In the scaling limit where the Bethe roots scale with the number of spin chain sites, the two loop Bethe equations in [1] can be recast as [9, 12, 14]

$$\frac{1}{z} + 2\pi n_u = 2\mathcal{G}_u - G_r \quad (3.1)$$

$$\frac{1}{z} + 2\pi n_v = 2\mathcal{G}_v - G_r \quad (3.2)$$

$$2\pi n_r = 2\mathcal{G}_r - G_v - G_u - G_w \quad (3.3)$$

$$2\pi n_w = G_r - G_s \quad (3.4)$$

$$2\pi n_w = 2\mathcal{G}_w - G_s \quad (3.5)$$

In these five equations z belongs to the several disjoint supports where the Bethe roots u, v, r, s, w condense, respectively. As usual

$$G_u = \sum_{j=1}^{M_u} \frac{1}{Lz - u_j}, \quad G_v = \sum_{j=1}^{M_v} \frac{1}{Lz - v_j}, \quad \dots \quad (3.6)$$

and the slash means the average of function above and bellow the cut resulting from the condensation of the Bethe roots. In this limit the spin chain can be described by a (super

symmetric) Landau-Lifshitz model and the corresponding algebraic curve can be compared with the curve described in the previous section. Indeed all the 5 nested Bethe equations nested can be turned into the statement that the quasimomenta

$$\begin{aligned}
q_1 = -q_{10} &= \frac{1}{z} - G_w \\
q_2 = -q_9 &= \frac{1}{z} + G_w - G_s \\
q_3 = -q_8 &= \frac{1}{z} - G_s + G_r \\
q_4 = -q_7 &= \frac{1}{z} - G_r + G_u + G_v \\
q_5 = -q_6 &= -G_u + G_v
\end{aligned} \tag{3.7}$$

form a ten-sheeted Riemann surface. The several properties of these quasimomenta follow trivially from the definition of the quasimomenta, see [9, 10, 11, 12, 13, 14]. This curve can be depicted as in figure 1 provided we drop the unit circle. The energy of the YM solutions is then given by

$$E = \sum_{i=1}^{M_u} \frac{\lambda^2}{u_i^2} + \sum_{i=1}^{M_v} \frac{\lambda^2}{v_i^2} \tag{3.8}$$

let us now consider the degeneration of the string previous algebraic curve in the Frolov-Tseytlin limit. In the spectral representation the analytical properties of the quasi-momenta q_i could be summarized in the following way (see [11, 12, 14] for similar decompositions) to the function strong coupling – see [6]. Finally let us mention that while in the AdS_5/CFT_4 we had a three loop mismatch here we the mismatch is obviously at leading order due to the function $f(\lambda)$ interpolating the dispersion relation between weak and strong coupling – see [6]. In the former case it was understood to be perfectly expectable and a generic feature of non commutative character the order of limits involved in the computations. Thus, here there is nothing worrisome about the mismatch being already at leading order. On the contrary, this is what we should expect in a generic situation.

Acknowledgments

We would like to thank J. Minahan and K. Zarembo for many useful discussions, for introducing us to the subject of integrability in the AdS_4/CFT_3 duality and for collaboration in earlier stages of this project. We are also grateful to V. Kazakov, I. Kostov, D. Serban and I. Shenderovich for useful comments. PV is funded by the Fundação para a Ciência e Tecnologia fellowship SFRH/BD/17959/2004/0WA9. NG was partially supported by RSGSS-1124.2003.2, by RFFI project grant 06-02-16786 and ANR grant INT-AdS/CFT (contract ANR36ADSCSTZ). A part of this work was done during NG’s stay at Les Houches Summer School, which he thanks for hospitality

References

- [1] J. A. Minahan and K. Zarembo, arXiv:0806.3951 [hep-th].
- [2] J. A. Minahan and K. Zarembo, JHEP **0303**, 013 (2003) [arXiv:hep-th/0212208].
- [3] O. Aharony, O. Bergman, D. L. Jafferis and J. Maldacena, arXiv:0806.1218 [hep-th].
- [4] J. H. Schwarz, JHEP **0411**, 078 (2004) [arXiv:hep-th/0411077]. • J. Bagger and N. Lambert, Phys. Rev. D **75**, 045020 (2007) [arXiv:hep-th/0611108]. • D. Gaiotto and X. Yin, JHEP **0708**, 056 (2007) [arXiv:0704.3740 [hep-th]]. • A. Gustavsson, arXiv:0709.1260 [hep-th]. • J. Bagger and N. Lambert, Phys. Rev. D **77**, 065008 (2008) [arXiv:0711.0955 [hep-th]]. • J. Bagger and N. Lambert, JHEP **0802**, 105 (2008) [arXiv:0712.3738 [hep-th]]. • M. Van Raamsdonk, JHEP **0805**, 105 (2008) [arXiv:0803.3803 [hep-th]]. • J. Distler, S. Mukhi, C. Papageorgakis and M. Van Raamsdonk, JHEP **0805**, 038 (2008) [arXiv:0804.1256 [hep-th]]. • P. M. Ho, Y. Imamura and Y. Matsuo, arXiv:0805.1202 [hep-th]. • J. Gomis, D. Rodriguez-Gomez, M. Van Raamsdonk and H. Verlinde, arXiv:0806.0738 [hep-th].
- [5] M. Benna, I. Klebanov, T. Klose and M. Smedback, arXiv:0806.1519 [hep-th]. • B. Ezhuthachan, S. Mukhi and C. Papageorgakis, arXiv:0806.1639 [hep-th]. • S. Cecotti and A. Sen, arXiv:0806.1990 [hep-th]. • A. Mauri and A. C. Petkou, arXiv:0806.2270 [hep-th]. • E. A. Bergshoeff, M. de Roo, O. Hohm and D. Roest, arXiv:0806.2584 [hep-th]. • P. de Medeiros, J. Figueroa-O'Farrill and E. Mendez-Escobar, arXiv:0806.3242 [hep-th]. • J. Bhattacharya and S. Minwalla, arXiv:0806.3251 [hep-th]. • M. Blau and M. O'Loughlin, arXiv:0806.3253 [hep-th]. • Y. Honma, S. Iso, Y. Sumitomo and S. Zhang, arXiv:0806.3498 [hep-th]. • Y. Imamura and K. Kimura, arXiv:0806.3727 [hep-th]. • A. Armoni and A. Naqvi, arXiv:0806.4068 [hep-th]. • A. Hanany, N. Mekareeya and A. Zaffaroni, arXiv:0806.4212 [hep-th]. • A. Agarwal, arXiv:0806.4292 [hep-th]. • C. Ahn, arXiv:0806.4807 [hep-th]. • J. Bedford and D. Berman, arXiv:0806.4900 [hep-th]. • K. Hosomichi, K. M. Lee, S. Lee, S. Lee and J. Park, arXiv:0806.4977 [hep-th]. • P. Fre and P. A. Grassi, arXiv:0807.0044 [hep-th]. • K. Okuyama, arXiv:0807.0047 [hep-th]. • N. Beisert, arXiv:0807.0099 [hep-th]. • J. Bagger and N. Lambert, arXiv:0807.0163 [hep-th]. • S. Terashima, arXiv:0807.0197 [hep-th]. • G. Grignani, T. Harmark, M. Orselli and G. W. Semenoff, arXiv:0807.0205 [hep-th].
- [6] T. Nishioka and T. Takayanagi, arXiv:0806.3391 [hep-th]. • D. Gaiotto, S. Giombi and X. Yin, arXiv:0806.4589 [hep-th]. • G. Grignani, T. Harmark and M. Orselli, arXiv:0806.4959 [hep-th].
- [7] B. . j. Stefanski, arXiv:0806.4948 [hep-th].
- [8] G. Arutyunov and S. Frolov, arXiv:0806.4940 [hep-th].
- [9] V. A. Kazakov, A. Marshakov, J. A. Minahan and K. Zarembo, JHEP **0405**, 024 (2004) [arXiv:hep-th/0402207].
- [10] V. A. Kazakov and K. Zarembo, JHEP **0410**, 060 (2004) [arXiv:hep-th/0410105].
- [11] N. Beisert, V. A. Kazakov and K. Sakai, Commun. Math. Phys. **263**, 611 (2006) [arXiv:hep-th/0410253].
- [12] S. Schafer-Nameki, Nucl. Phys. B **714**, 3 (2005) [arXiv:hep-th/0412254].

- [13] N. Beisert, V. A. Kazakov, K. Sakai and K. Zarembo, *Commun. Math. Phys.* **263**, 659 (2006) [arXiv:hep-th/0502226].
- [14] N. Beisert, V. A. Kazakov, K. Sakai and K. Zarembo, *JHEP* **0507**, 030 (2005) [arXiv:hep-th/0503200].
- [15] I. Bena, J. Polchinski and R. Roiban, *Phys. Rev. D* **69** (2004) 046002 [arXiv:hep-th/0305116].
- [16] N. Gromov and P. Vieira, *Nucl. Phys. B* **789** (2008) 175 [arXiv:hep-th/0703191].
- [17] D. E. Berenstein, J. M. Maldacena and H. S. Nastase, *JHEP* **0204** (2002) 013 [arXiv:hep-th/0202021].
- [18] N. Gromov and P. Vieira, *Nucl. Phys. B* **790** (2008) 72 [arXiv:hep-th/0703266]. • N. Gromov and P. Vieira, *JHEP* **0804** (2008) 046 [arXiv:0709.3487 [hep-th]]. • N. Gromov, S. Schafer-Nameki and P. Vieira, arXiv:0801.3671 [hep-th].
- [19] N. Beisert, *Nucl. Phys. B* **676**, 3 (2004) [arXiv:hep-th/0307015]. • N. Beisert, J. A. Minahan, M. Staudacher and K. Zarembo, *JHEP* **0309**, 010 (2003) [arXiv:hep-th/0306139]. • N. Beisert and M. Staudacher, *Nucl. Phys. B* **670**, 439 (2003) [arXiv:hep-th/0307042]. • N. Beisert, C. Kristjansen and M. Staudacher, *Nucl. Phys. B* **664**, 131 (2003) [arXiv:hep-th/0303060]. • N. Beisert, V. Dippel and M. Staudacher, *JHEP* **0407**, 075 (2004) [arXiv:hep-th/0405001]. • M. Staudacher, *JHEP* **0505** (2005) 054 [arXiv:hep-th/0412188]. • G. Arutyunov, S. Frolov and M. Staudacher, *JHEP* **0410** (2004) 016 [arXiv:hep-th/0406256]. • N. Beisert and M. Staudacher, *Nucl. Phys. B* **727**, 1 (2005) [arXiv:hep-th/0504190]. • N. Beisert, “The $su(2-3)$ dynamic spin chain,” *Nucl. Phys. B* **682**, 487 (2004) [arXiv:hep-th/0310252]. • N. Beisert, B. Eden and M. Staudacher, *J. Stat. Mech.* **0701**, P021 (2007) [arXiv:hep-th/0610251]. • N. Beisert, R. Hernandez and E. Lopez, *JHEP* **0611**, 070 (2006) [arXiv:hep-th/0609044].